Achromatic Optical Vortex Coronagraph with Subwavelength Gratings

Dimitri Mawet[1], Pierre Riaud[1,2], Jacques Baudrand[2], Anthony Boccaletti[2], Pierre Baudoz[2], Daniel Rouan[2], Cédric Lenaerts[3], and Jean Surdej[1]

[1]*Institut d'Astrophysique et de Géophysique de Liège (IAGL), University of Liège,*
[2] *LESIA, Observatory of Paris-Meudon,*
[3] *HOLOLAB, Department of physics, University of Liège*

ABSTRACT

We present in this short paper an efficient and powerful solution for making achromatic optical vortex coronagraphs. We propose to use the unique properties of subwavelength grating integrated meta-materials to induce achromatic phase shifts that can be implemented to yield vortices of any topological charge. TPF-C specifications are very challenging and require pushing this concept to its limits.

1. INTRODUCTION

Optical vortices have recently gained interest in the coronagraphists community (see the papers from Palacios and Swartzlander, these proceedings). Such an attraction is comprehensible since they present many advantages over other concepts of coronagraphs like for example, the conjunction of high rejection ratios, small inner working distance, full discovery space, high throughput, etc. In the framework of ground-based coronagraphy for second-generation instrumentation, they are foreseen to advantageously replace classical Lyot coronagraphs, and even more recent coronagraphs such as the four-quadrant phase-mask coronagraph which is already online at the VLT (Boccaletti et al. 2004, Riaud et al. 2006). For TPF-C, where the detectivity constraints are dramatically emphasized, optical vortices represent a competitive approach. Nevertheless, in order to be compliant with the daunting specifications of an Earth-like planet-finding mission like TPF-C, one has to push the concept to its limits. Two major problems are to be solved before seriously considering the implementation of optical vortices into this ambitious space observatory. First of all, their sensitivity to low-order aberrations has to be significantly kept below an acceptable level for the telescope pointing stability constraint to remain in comfortable margins. This issue also relates to the sensitivity to stellar angular diameter which is known to dramatically affect small inner working distance coronagraphs such as the FQPM, for instance (Guyon et al. 2006). Finally, as optical vortices are phase masks, one has to find a way to efficiently achromatize them, i.e., making them keeping their high rejection ratios over wavelength ranges equivalent to the usual astrophysical filters (bandwidth of ~ 20 %).

2. SUBWAVELENGTH GRATINGS

When the period of a grating is smaller than the wavelength of the incident light, it does not diffract as a classical spectroscopic grating. All the incident energy is enforced to propagate only in the zeroth order, leaving incident wavefronts free from any further aberrations. The subwavelength gratings are therefore often called Zeroth Order Gratings (ZOGs). This type of gratings behaves like homogeneous media with unique characteristics, which can be used to synthesize artificial birefringent achromatic waveplates. Quarterwave or halfwave plates are extensively used in astrophysics for polarimetric studies. Subwavelength gratings constitute an elegant, flexible and integrated solution to produce them. The key point is that by carefully controlling the geometry of the grating structure, one can tune the so-called form birefringence and induce a precise phase shift between the orthogonal polarization components of the incident light. The phase shifting optical function can then be integrated at the surface of a substrate with any kind of geometry (Figure 1), leading to an efficient and flexible solution for implementing the phase shifting spatial distribution of phase-mask coronagraph such as the FQPM (Mawet et al. 2005a) or the AGPM (Mawet et al. 2005b).

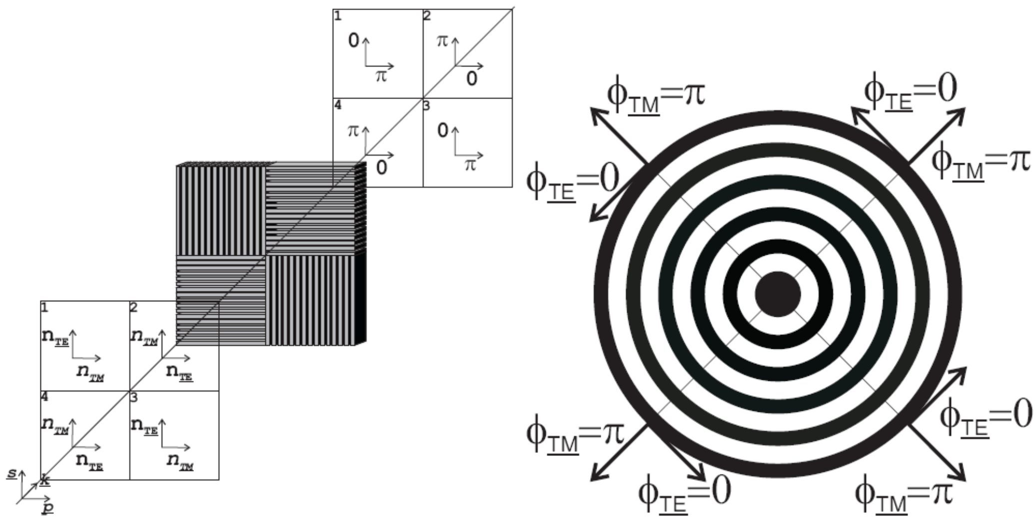

Figure 1: *Left: 4QZOG implementation (Mawet et al. 2005a), where the four subwavelength gratings engraved on a unique substrate are strictly identical and implemented in the following way: 2 of them in 2 quadrants along 1 diagonal are rotated by 90° around their normals with respect to the two others. Right: AGPM implementation (Mawet et al. 2005b). The AGPM consists of a concentric circular surface-relief grating with rectangular grooves with depth h and a periodicity Λ. It can be seen as a circularly symmetric FQPM in polarization.*

3. LIMITATIONS OF THE ANNULAR GROOVE PHASE MASK CORONAGRAPH

The AGPM is an optical vortex of topological charge 2 (Mawet et al. 2005b). It can be demonstrated that the sensitivity to a low-order optical aberration x depends on the topological charge m as x^m (Mawet et al. 2005b). This sensitivity to low-order aberrations is the harmful counterpart of the property of small inner working distance of this coronagraph and others like the FQPM or the AIC, for instance. This side-effect is too penalizing to consider the AGPM directly as such for TPF-C. It is however worth noting that, by adding a tiny Lyot dot at the center, this effect can be reduced together with the sensitivity to the stellar size (Mawet et al. 2005b). As far as the achromatization is concerned, one can expect total nulling depths of about 5×10^{-6} over 20% bandwidths (without the central Lyot dot). This means that the contrast at an angular separation of 4 λ/D can reach about 5×10^{-8} in the unaberrated case. This is still more than 2 orders of magnitude above the required 10^{-10} specification imposed by the contrast between an Earth-like planet in the habitable zone and its host star. The 5×10^{-8} limit is not fundamental but design-dependent which also means technology-dependent.

4. HIGHER-ORDER MASKS

Higher-order masks must be investigated for TPF-C. A compromise between the IWD and aberration sensitivity must be found. According to Guyon et al. 2006, an m=6 vortex mask would be the better compromise for TPF-C. Achieving such a topological charge with subwavelength gratings only depends on our ability to control the orientation of the grating lines to be imprinted (Figure 2). In this context, state-of-the-art realizations (see e.g., Niv et al. 2006) have already achieved m=4 masks without any difficulty in the infrared (10.6 microns) and on top of AsGa substrates (Figure 2).

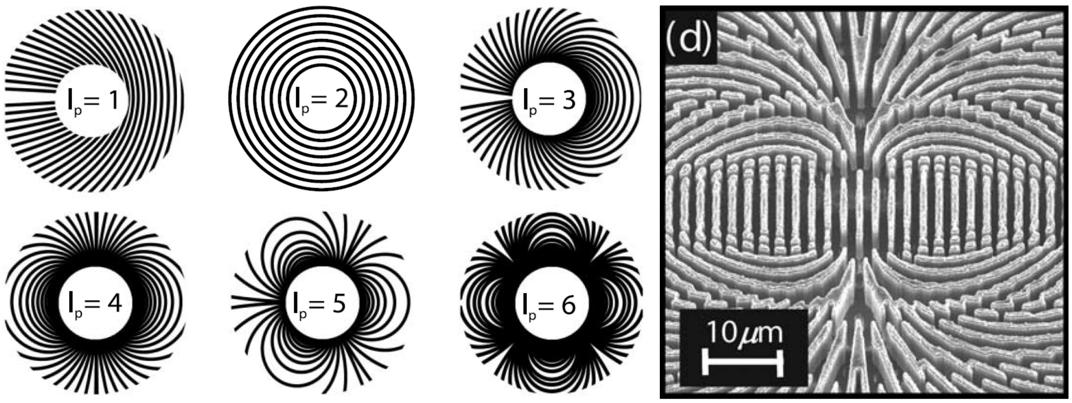

Figure 2: *Left: grating geometry for different topological charges (1-6). Right: SEM picture of a realization by Erez Hasman's group (Israel Institute of Technology). This picture shows an m=4 optical vortex engraved in an AsGa substrate for infrared applications (10.6 microns).*

5. VISIBLE OPERATION

Making subwavelength gratings for the visible wavelength range is not trivial. Subwavelength means that the period of the grating must be smaller than the wavelength of the incident light. In the visible, this means that the period of the grating must absolutely be smaller than λ/n, n being the index of refraction of the chosen substrate material. We therefore have to deal with periods in the 300 to 400 nm range according to the material. Controlling the micro-structure at such scales is challenging but feasible using for instance nano-imprint lithography techniques. In this context, let us cite the work of Deng et al. (2005) for optical pickup units. They indeed proposed, manufactured and tested (now commercialize) achromatic subwavelength grating waveplates for the visible. Converting the performance of their manufactured components (Figure 3) in terms of nulling efficiency would lead to a mere 1000 rejection ratio over a bandwidth of more than 20 %. There is still room for improvement. An intensive research in the grating optimization for the visible is nevertheless needed.

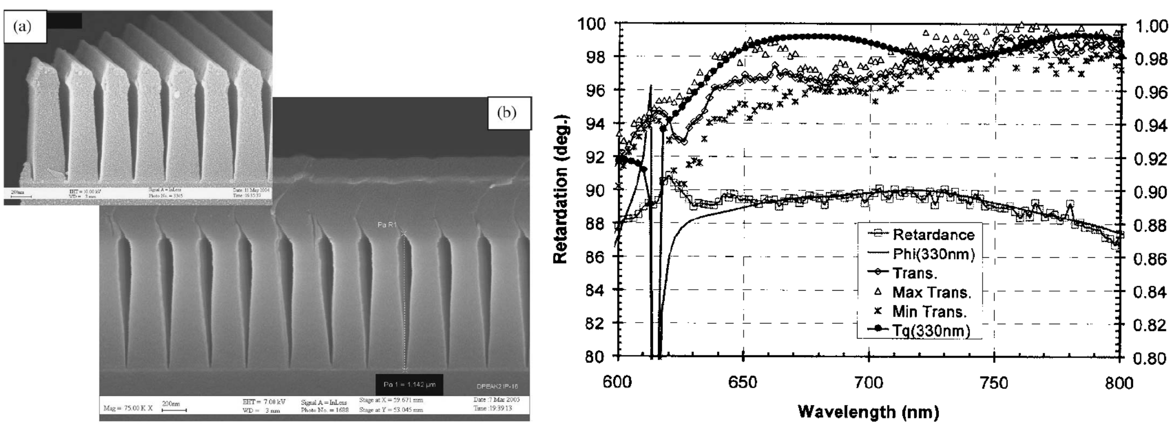

Figure 3: *Left: SEM picture of a subwavelength grating achromatic phase shifter for the visible. Right: measured performance of the micro-structure in terms of phase and throughput over the visible (Deng et al. 2005)*

6. CHROMATIC RESIDUALS FILTERING

Assuming a state-of-the-art nulling performance of 5×10^{-6} over a 100 nm bandwidth in the visible from the subwavelength grating technology, i.e., a contrast of about 5×10^{-8} at 4 λ/D in the unaberrated case, this imposes us to gain an additional factor of 1000 to reach the required level of 10^{-10}. If we consider the vectorial nature of the vortex induced by the space-variant grating (see Niv et al. 2006, for instance), we can use the Jones formalism that gives the following matrix for the transmission through the component, in the helical basis:

$$J_{vortex}(x,y) = \frac{1}{2}\left(\eta_{TE} + \eta_{TM} e^{i\Delta\phi}\right)\begin{bmatrix} 1 & 0 \\ 0 & 1 \end{bmatrix} + \frac{1}{2}\left(\eta_{TE} - \eta_{TM} e^{i\Delta\phi}\right)\begin{bmatrix} 0 & e^{i2\theta} \\ e^{-i2\theta} & 0 \end{bmatrix}$$

This equation indicates that the field emerging from a space-variant subwavelength grating comprises three components. The first (left term) maintains the original polarization state and phase of the incoming beam. The second (right term, top right component) is right-handed circularly polarized and has a phase modification of $2\theta(x,y)$, inducing a vortex of topological charge m according to the adopted geometry ($\theta(x,y)$ defines the orientation of the grating grooves, see Figure 2) . The third (right term, down left component) has an orthogonal polarization direction and opposite phase modification with respect to the second component. Note that the magnitude of the different components is determined by the local birefringent parameters of the subwavelength gratings: the diffraction efficiencies in transmission for the polarization components TE (or s) and TM (or p) η_{TE}, η_{TM} and the phase shift between them $\Delta\Phi$. The transmission of subwavelength dielectric gratings is relatively high and the retardation $\Delta\Phi$ is primarily a function of the subwavelength groove geometry (filling factor) and etching depth. The ideal situation is for η_{TE}, $\eta_{TM}=1$ and $\Delta\Phi=\pi$. Unfortunately, this idyllic behaviour cannot be maintained over large bandwidths and lead in practice to the 5×10^{-6} over 20 % bandpass limitation mentioned here above. However, any departure from the perfect conditions will result into a *transfer of energy* between the circularly polarization states with the embedded optical vortex and the first term that conserves the original polarization state (free of the optical singularity). This crucial property of vectorial vortices, and vectorial vortices only, allows us to consider splitting and filtering the polarization. This splitter/filter should induce an extinction ratio of 1000 or more, corresponding to the additional factor needed to reach the 10^{-10} contrast at 4 λ/D. A proper data post processing with both polarizations could also help increasing the contrast to reach 10^{-10} at 4 λ/D by calibrating the residual speckles. In practice, the polarization filter/splitter only consists in quarterwave plates and linear polarizing filters/beamsplitters. Note that the subwavelength grating technology could synthesize both components, and with the advantage that the whole optical function could be integrated on top of a single substrate (Deguzman & Nordin 1999).

7. CONCLUSIONS

Optical vortices such as the AGPM are promising coronagraphs for ground-based applications of extrasolar planet-finding instruments. In particular, we are currently manufacturing prototypes for the VLT-Planet Finder second-generation XAO instrument for the VLT (SPHERE). Optical vortices of higher orders are well ranked for TPF-C. However, manufacturing them at the required specification for Earth-like planet detection is extremely challenging. In this paper, we have reviewed the current state of the art of the vectorial vortex technology. Vectorial vortices are induced by space-variant subwavelength gratings. Pushing this technology to its limits, we proposed some hints to reach the 10^{-10} over usable bandwidths. This however would require further studies to definitely conclude on the feasibility of the proposed concept for TPF-C.

REFERENCES

Boccaletti et al. 2004, PASP 116, 1061
Deguzman & Nordin 1999, Appl. Opt. 40, 5731
Deng et al. 2005, Optics Letters 30, 2614
Guyon et al. 2006, submitted to ApJ
Mawet et al. 2005a, Appl. Opt. 44, 7313
Mawet et al. 2005b, ApJ 633, 1191
Niv et al. 2006, Opt. Express 14, 4208
Riaud et al. 2006, A&A 458, 317